JOURNAL OF CATALYSIS 130, 411–422 (1991)

Acidity/Basicity of Rare-Earth Oxides and Their Catalytic Activity in Oxidative Coupling of Methane to C_2-Hydrocarbons

V. R. CHOUDHARY[1] AND V. H. RANE

Chemical Engineering Division, National Chemical Laboratory, Pune-411 008, India

Received August 17, 1990; revised January 23, 1991

Rare-earth metal oxides (viz. La_2O_3, CeO_2, Sm_2O_3, Eu_2O_3, and Yb_2O_3) have been compared for their acid and base strength distribution (measured by stepwise thermal desorption of CO_2 from 323 to 1173 K and TPD of NH_3 from 323 to 1223 K, respectively) and their catalytic activity/selectivity in oxidative coupling of methane to C_2-hydrocarbons at 973–1123 K (space velocity = 108,000 $cm^3 \cdot g^{-1} h^{-1}$ and $CH_4/O_2 = 4$ and 8). The catalyst activity and selectivity showed dependence on both the surface acidity and basicity. However, the relationship of the catalytic activity/selectivity with the surface acidity/basicity is not straightforward; it is quite complex. Stronger acid sites are found to be harmful for the selectivity. There is a possibility of an involvement of an acid–base pair (M^{n+}_{LC} O^{2-}_{LC}, where subscript LC denotes low coordination) on the surface in the abstraction of the H-atom from adsorbed methane molecule by its polarization followed by heterolytic C–H bond rupture to form CH_3^- (which interacts with M^{n+}_{LC}) and $(OH)^-_{LC}$ and a transfer of electron from the carbanion to O_2, resulting methyl radical and O_2^-. Regeneration of basic sites and the possibility of formation of O^- species on the catalyst surface are discussed.

INTRODUCTION

A number of studies have been reported on oxidative coupling of methane to C_2-hydrocarbons over rare-earth oxides (*1–7*) and rare-earth-promoted alkaline earth oxides (*8–10*). Oxidative coupling of methane is carried out at high temperatures (973–1173 K). Because of their high melting points, rare-earth oxides are superior in thermal stability to catalysts containing low melting metal oxides/salts for the methane coupling process.

Otsuka *et al.* (*1, 3*) observed that, among rare-earth oxides, Sm_2O_3 shows highest activity and selectivity for C_2-hydrocarbons in the oxidative coupling of methane. Whereas Campbell *et al.* (*5*) have found that for hydrothermally treated rare-earth oxides, La_2O_3 shows much higher activity than Sm_2O_3 in catalytic production of gas-phase methyl radicals from methane and also in oxidative coupling of methane. However, in both the studies, CeO_2 showed very low activity/selectivity in the methane coupling process. It was pointed out that the relative activities of rare-earth metal oxides parallel their basicities (*5*). It is, therefore, very interesting to know quantitatively the surface basicity and base strength distribution on rare-earth oxides. The catalytic activity/selectivity of rare-earth oxides may also be influenced by their surface acidity. It is, therefore, of great interest to know the influence of both the basicity and acidity of the catalysts on their activity and selectivity in oxidative coupling of methane.

The present investigation was undertaken with the objectives of studying the basicity/base strength distribution (by stepwise thermal desorption of CO_2) and acidity distribution (by temperature-programmed desorption of NH_3) on rare-earth oxides (viz. La_2O_3, CeO_2, Sm_2O_3, Eu_2O_3, and Yb_2O_3) and finding the relationship between their

[1] To whom correspondence should be addressed.

0021-9517/91 $3.00

surface acidity/basicity and catalytic activity/selectivity in oxidative coupling of methane to C_2-hydrocarbons.

EXPERIMENTAL

The catalysts were prepared from high purity (99.9%) rare-earth oxides (viz. La_2O_3, CeO_2, Sm_2O_3, Eu_2O_3, and Yb_2O_3) by hydrothermal treatment followed by high temperature calcination, as follows. Powdered rare-earth oxide was treated with deionized water (3 ml water per gram of the rare-earth oxide) on water bath for 4 h while maintaining the water content of the slurry constant. The slurry was dried overnight at 393 K. The dried mass was pressed and crushed to 22 to 30-mesh size particles and then calcined in static air at 873 K for 6 h.

Before carrying out measurements on their surface area, acidity, basicity, and catalytic activity, the catalysts were calcined *in situ* at 1223 K in a flow of moisture-free helium (20 $cm^3 \cdot min^{-1}$) for 2 h.

The surface area of the catalysts (precalcined at 1223 K as above) was determined by the single-point BET method by measuring the adsorption of nitrogen (conc. of N_2: 30 mol% balance helium) at liquid nitrogen temperature, using Monosorb surface area analyser (Quanta Chrome Corp.).

The basicity and base strength distribution on the catalysts (pretreated *in situ* at 1223 K as above) were determined by the stepwise thermal desorption (STD) of CO_2 with evolved gas analysis (*11*). The STD of CO_2 was carried out by desorbing the CO_2 chemisorbed at 323 K on the catalyst (about 1.0 g, packed in a quartz reactor) in the flow of He (20 $cm^3 \cdot min^{-1}$) by heating it from 323 to 1173 K in a number of successive temperature steps (323–423 K, 423–573 K, 573–773 K, 773–1173 K). When the maximum temperature of the respective step was attained, it was maintained for a period of 30 min to desorb the CO_2 reversibly adsorbed on the catalyst at that temperature. The amount of CO_2 desorbed in each step was determined gravimetrically by absorbing it completely in an aqueous barium hydroxide solution. The detailed procedure for measuring the base strength distribution by the STD of CO_2 has been described earlier (*11*).

The acidity of the catalyst was determined by temperature-programmed desorption (TPD) of ammonia (chemisorbed at 373 K) in a quartz reactor from 323 to 1223 K at a linear heating rate of 20 $K \cdot min^{-1}$ in a flow of helium (20 $cm^3 \cdot min^{-1}$). Before the collection of TPD data, the catalyst (0.5 g) packed in the quartz reactor was calcined *in situ* at 1223 K for 2 h in a flow of helium (20 $cm^3 \cdot min^{-1}$). The chemisorption of ammonia at 373 K was carried out by saturating the catalyst by ammonia and desorbing the physically adsorbed ammonia at 373 K in the flow of helium for 30 min. The ammonia desorbed in the TPD was detected by a thermal conductivity detector. The ammonia chemisorbed at 373 K was determined quantitatively by absorbing in dilute HCl the ammonia desorbed in the TPD run and determining the HCl consumed by titration.

Throughout this paper, the chemisorption is considered as the amount of adsorbate retained by the presaturated catalyst after it was swept with pure helium for a period of 30 min.

Oxidative coupling of methane over the catalysts was carried out at atmospheric pressure in a conventional flow quartz reactor (i.d. 10 mm) packed with 0.1 g catalyst. The reaction temperature was measured by a chromel–alumel thermocouple located in the catalyst bed. Before the reaction, the catalyst was pretreated *in situ* in the flow of He (20 $cm^3 \cdot min^{-1}$) at 1223 K for 2 h. The feed consists of only methane and oxygen. The performance of the catalyst in the reaction was studied at the following experimental conditions: amount of catalyst, 0.1 g; feed gas flow rate, 180 $cm^3 \cdot min^{-1}$ (at STP) or 108,000 $cm^3 \cdot g^{-1} \cdot h^{-1}$; CH_4/O_2 ratio in feed, 4 and 8; and temperature, 973–1123 K. The reactor effluent gases, after removal of water by condensation, were analysed by an on-line gas chromatograph using Porapak-Q and Spherocarb columns.

High purity gases He (>99.99%), CH_4 (99.995%), CO_2 (99.995%), O_2 (99.5%), and

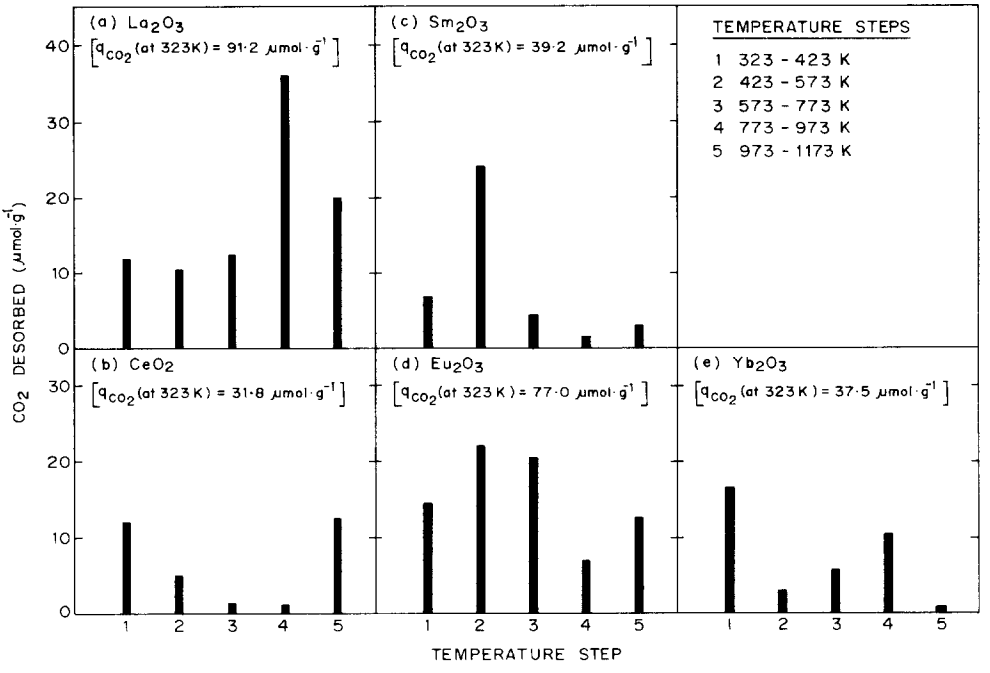

FIG. 1. Step-wise thermal desorption of CO_2 on the rare earth metal oxide catalysts from 323-1173 K (q_{CO_2} = amount of CO_2 chemisorbed).

NH_3 (99.99%) were used in the above experimental work.

RESULTS

STD of CO_2

The basicity and base strength distribution on the rare-earth oxide catalysts (calcined at 1223 K) under conditions close to those of their operation have been determined by the STD of CO_2 from 323–1173 K.

The base strength distribution on the catalysts is presented in Fig. 1. The columns in the figure show the energy distribution of the sites involved in the chemisorption of CO_2 at the lowest temperature of the STD (i.e., 323 K). Each column represents the number of sites measured in terms of CO_2 desorbed in the corresponding temperature step. The strength of these sites is expressed in terms of the desorption temperature of CO_2, Td, which lies in the range in which the CO_2 chemisorbed at the lowest temperature of the step is desorbed. The sites of strength $T_1 < Td \leq T_2$ could be obtained from the amount of CO_2 which was initially chemisorbed at T_1 and subsequently desorbed when the temperature was increased from T_1 to T_2.

The temperature dependence of the chemisorption of CO_2 on the catalysts (obtained from the STD data) is shown in Fig. 2. The chemisorption of CO_2 at a higher tempera-

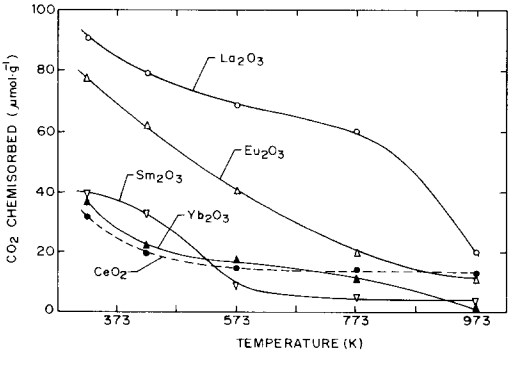

FIG. 2. Chemisorption of CO_2 on the rare earth metal oxide catalysts at different temperatures.

ture points to an involvement of stronger sites. The CO_2 chemisorption vs temperature curves, therefore, presents the type of site energy distribution in which the number of sites are expressed in terms of the amount of CO_2 chemisorbed as a function of chemisorption temperature.

The results (Figs. 1 and 2) indicate that the catalysts have broad site energy distribution for their basic sites and also differ from each other widely in their total basicity (measured in terms of the CO_2 chemisorbed at 323 K) and base strength distribution.

TPD of Ammonia

The acid strength distribution on the catalysts was studied by the TPD of ammonia (chemisorbed on the catalysts at 373 K) from 323 to 1223 K at a heating rate of 20 $K \cdot min^{-1}$ using helium as a carrier gas.

The TPD curves for the catalysts along with their initial surface coverage (θi) by the ammonia chemisorbed at 373 K are presented in Fig. 3. The distribution of acid sites on the CeO_2, Sm_2O_3, Eu_2O_3, and Yb_2O_3 catalysts is very broad, whereas that of the La_2O_3 catalyst is relatively narrow. For the catalysts other than La_2O_3, the TPD peaks exist in the region of lower temperatures and also at higher temperatures (Fig. 3b–3e). This shows the presence of both the weak and strong acid sites on these catalysts, whereas the TPD curve in Fig. 3a indicates the presence of only intermediate strength acid sites on the La_2O_3 catalyst. The results reveal that the catalysts differ from each other widely in their total number of acid sites (measured in terms of the chemisorption of ammonia at 373 K) and also in the site energy distribution of the acid sites.

Oxidative Coupling of Methane

Results showing the influence of temperature (973–1123 K) and CH_4/O_2 ratio in the feed (CH_4/O_2 = 4 and 8) on the methane conversion, selectivity for the C_2-hydrocarbons and ethylene/ethane ratio in products in the oxidative coupling of methane over the catalysts are presented in Figs. 4–9.

In case of the La_2O_3 catalyst for CH_4/O_2 = 4, the increase in the temperature does not affect significantly the methane conversion but causes a small decrease in the C_2-selectivity (Fig. 4a). However, for the higher CH_4/O_2 ratio (8.0), both the conversion and the C_2-selectivity (and consequently the C_2-yield) are increased with the temperature (Fig. 4b). The increase in the CH_4/O_2 ratio results in a decrease in the selectivity at the lower temperature (973 K) but an increase in the selectivity at the higher temperatures ($\geq$1023 K).

The CeO_2 catalyst shows a very poor C_2-selectivity at all the temperatures and CH_4/O_2 ratios (Fig. 5). However, both the conversion and the selectivity are increased with the temperature.

For the Sm_2O_3 catalyst, at CH_4/O_2 = 8 both the conversion and the C_2-selectivity (and hence the C_2-yield) are increased with the temperature (Fig. 6b). However, at the lower CH_4/O_2 ratio (4.0), the conversion is increased to a very small extent and the selectivity is passed through a maximum with the increase in the temperature; the change in the selectivity, particularly above 1023 K, is small. The catalyst shows higher C_2-selectivity at the higher CH_4/O_2 ratio.

In case of the Eu_2O_3 catalyst, when the temperature is increased the selectivity (except for CH_4/O_2 = 4) and the conversion are increased. However, the selectivity at the CH_4/O_2 ratio = 4 is passed through a maximum (Fig. 7).

The Yb_2O_3 catalyst shows poor methane conversion (Fig. 8). On this catalyst, both the conversion and the selectivity are increased with the temperature.

For all the catalysts, the ethylene/ethane ratio is higher for the lower CH_4/O_2 ratio (or at higher O_2 concentration) and it is increased to a large extent with the increase in the temperature (Figs. 4–8).

Figure 9 shows the effect of temperature and CH_4/O_2 ratio (in the feed) on the CO/CO_2 ratio in the products of the oxidative methane coupling process. For all the catalysts, the CO/CO_2 ratio is higher at the

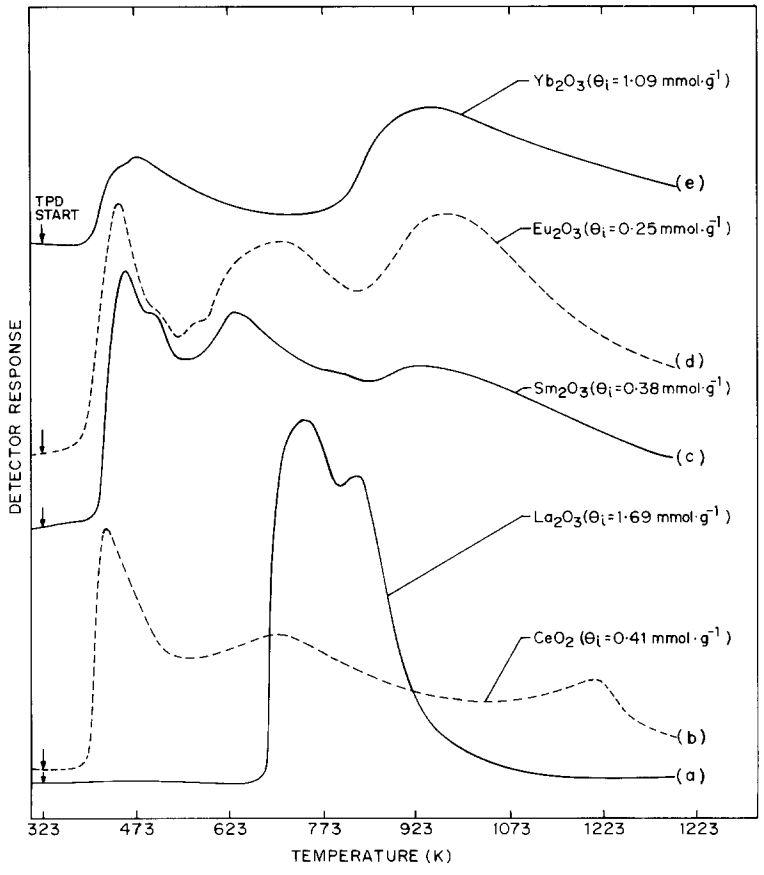

FIG. 3. TPD of ammonia on the rare earth metal oxide catalysts (θi = initial surface coverage by the NH_3 chemisorbed at 373 K).

higher CH_4/O_2 ratio (i.e., at the lower O_2 concentration). Among the catalysts, the Yb_2O_3 shows highest CO/CO_2 ratio, whereas the CeO_2 shows the lowest CO/CO_2 ratio.

In the absence of catalyst (or in the empty reactor), the conversion of methane for the CH_4/O_2 of 4.0 and 8.0 was $\leq$ 0.4 and 0.2%, respectively. This shows that the conversion of methane by its homogeneous oxidation with O_2 in the gas phase is negligibly small as compared to the oxidative conversion of methane over the rare-earth oxides studied.

Comparison of Catalysts

For the purpose of comparison of the catalysts, the data on their activity/selectivity in the oxidative coupling of methane (at 1223 K and CH_4/O_2 = 4 and 8) along with their surface properties (viz. surface area, surface basicity measured in terms of the CO_2 chemisorbed at 323 K, strong basic sites measured in terms of the CO_2 chemisorbed at 773 K, and surface acidity measured in terms of the NH_3 chemisorption at 373 K) are presented in Table 1.

Among the rare-earth oxide catalysts studied, the highest C_2-selectivity and C_2-yield are shown by the La_2O_3 catalyst, whereas the lowest selectivity and yield are observed for the CeO_2 catalyst. The order of the La_2O_3, Sm_2O_3, and CeO_2 for their activity/selectivity is consistent with that observed by Campbell *et al.* (5) for hydrothermally treated rare-earth oxides. How-

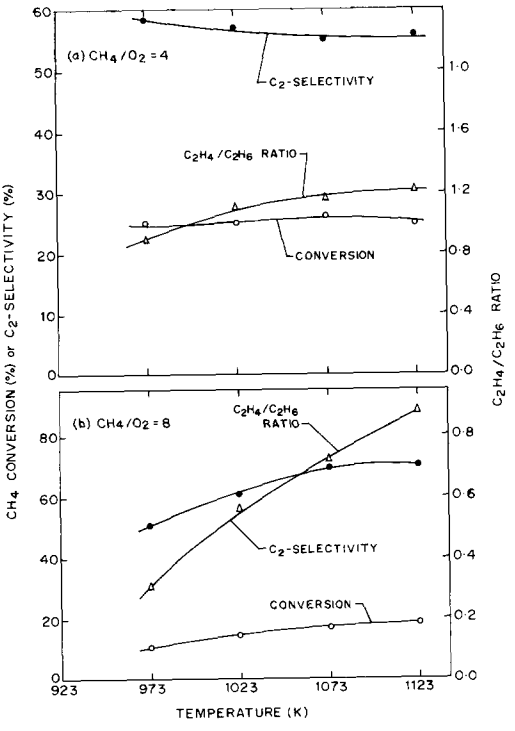

FIG. 4. Dependence of CH_4 conversion, C_2-selectivity and ethylene/ethane ratio in oxidative coupling of methane over the La_2O_3 on reaction temperature and CH_4/O_2 ratio.

ever, Otsuka *et al.* (*1*, *3*) observed lowest activity/selectivity for CeO_2 but highest activity/selectivity for Sm_2O_3 instead of La_2O_3. The hydrothermal treatment given to La_2O_3 and Sm_2O_3 may be responsible for the change in their order for the activity/selectivity. Korf *et al.* (*7*) have observed a large drop in both the activity and C_2-selectivity of Sm_2O_3 due to a change in its crystal structure from cubic to monoclinic. Above 1173 K, Sm_2O_3 exists in monoclinic form. In the present case, the calcination temperature of Sm_2O_3 was 1223 K. This may also be a reason for the observed difference between the results of this work and those of Otsuka *et al.* (*1*).

The La_2O_3 catalyst showed highest surface basicity and strong basic sites, whereas the CeO_2 and Sm_2O_3 catalysts showed lowest surface basicity and strong basic sites, respectively. The La_2O_3 catalyst also showed highest surface acidity but all of its acid sites are of intermediate strength. However, both the weak and strong acid sites are present on the Yb_2O_3, Eu_2O_3, Sm_2O_3, and CeO_2 catalysts. The strongest acid sites are observed on the CeO_2 catalyst.

DISCUSSION

Surface Acidity and Basicity

The acidity and basicity distributions studies reveal the presence of site energy distributions or group of sites of different energies on the rare-earth oxides studied. The acidity and basicity are attributed to the cations (M^{n+}) and anions (O^{2-}), respectively, exposed on the surface of the catalysts. The acid strength (or electron pair acceptor (EPA) strength) of the surface sites is expected to be dependent upon the effective $+ve$ charge on the metal cations and/or their coordination on the catalyst surface. Similarly, the base strength (or electron pair donor (EPD) strength) of the surface sites is

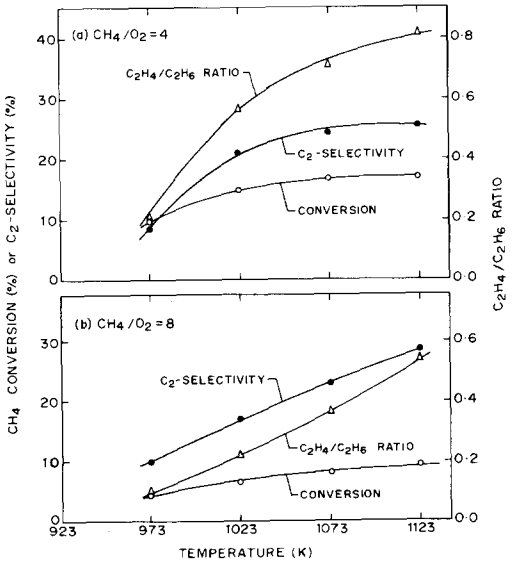

FIG. 5. Dependence of CH_4 conversion, C_2-selectivity and ethylene/ethane ratio in oxidative coupling of methane over the CeO_2 on reaction temperature and CH_4/O_2 ratio.

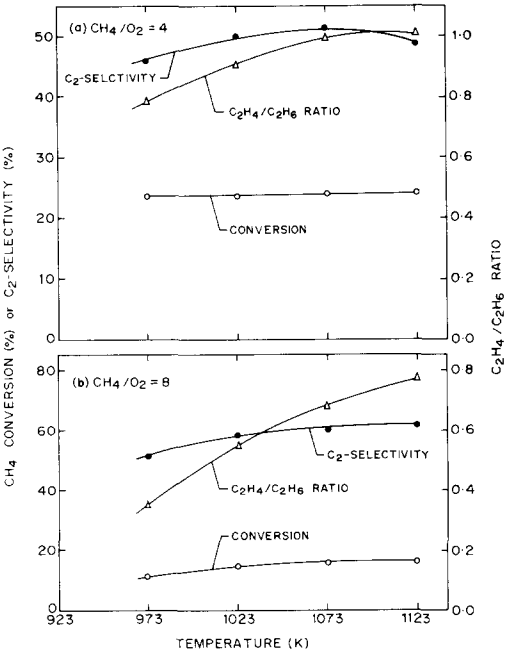

FIG. 6. Dependence of CH_4 conversion, C_2-selectivity and ethylene/ethane ratio in oxidative coupling of methane over the Sm_2O_3 on reaction temperature and CH_4/O_2 ratio.

also expected to vary depending upon the effective $-ve$ charge on the anions and/or their coordination on the surface. Surface imperfections such as steps, kinks, corners, which provide sites for ions of low coordination M^{n+}_{LC} and O^{2-}_{LC}, are expected to be responsible for the presence of sites of different strengths (*12*).

Catalytic Activity/Selectivity

The methane conversion and C_2-yield obtained on the catalysts are in the order ($La_2O_3 > Sm_2O_3 > CeO_2$) which is consistent with that observed by Campbell *et al.* (*5*). The observed catalyst order is also consistent with the order for their rate of methyl radical formation (*6*). The C_2-selectivity and yield observed for the La_2O_3 is higher than that observed for the other rare-earth oxides studied in which the metal can exist in two oxidation states. This confirms the earlier observation (*5*) that metal centres with multiple stable oxidation states are not necessarily required for the catalytic activity/selectivity. Further, the lowest C_2-selectivity and yield observed for the CeO_2 is very much consistent with the earlier observation (*6*) that methyl radicals react extensively with CeO_2, leading to their conversion to CO_2, whereas they react only to a small extent with La_2O_3, Sm_2O_3, Eu_2O_3, and Yb_2O_3. Also, the lowest methane conversion activity of Yb_2O_3 is consistent with the fact that it is intrinsically a poor radical former (*6*).

For all the rare-earth oxides studied (except for the La_2O_3) when $CH_4/O_2 = 4.0$ and the Sm_2O_3 and Eu_2O_3 above 1073 K when $CH_4/O_2 = 4.0$, the C_2-selectivity is increased with the temperature. The increase in the C_2-selectivity may be due to a decrease in the formation of CO and CO_2 from methyl radicals by gas-phase reaction (*13*);

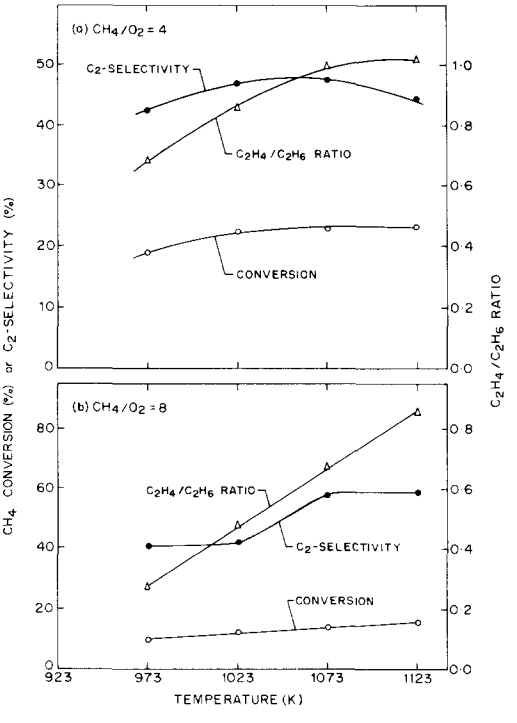

FIG. 7. Dependence of CH_4 conversion, C_2-selectivity and ethylene/ethane ratio in oxidative coupling of methane over the Eu_2O_3 on reaction temperature and CH_4/O_2 ratio.

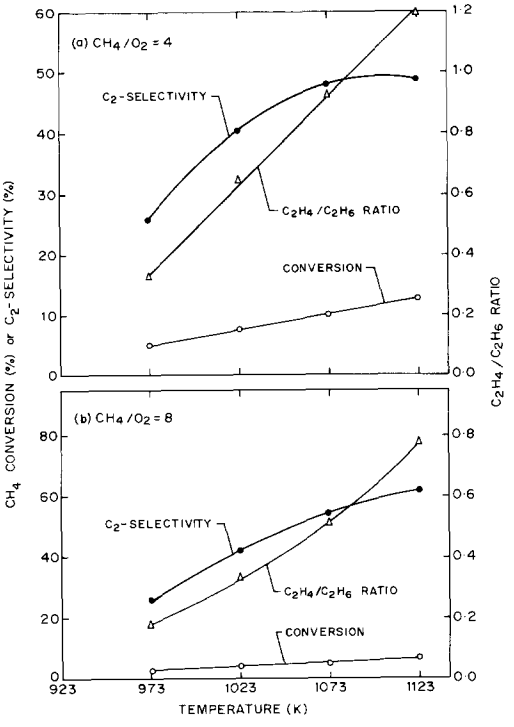

FIG. 8. Dependence of CH_4 conversion, C_2-selectivity and ethylene/ethane ratio in oxidative coupling of methane over the Yb_2O_3 on reaction temperature and CH_4/O_2 ratio.

$$CH_3. + O_2 \rightleftarrows CH_3O_2. \rightarrow \rightarrow CO, CO_2 \quad (1)$$

The formation of methyl peroxy radicals ($CH_3O_2.$), which leads to CO and CO_2, is not favoured at higher temperatures (*2, 13*) and hence the C_2-selectivity is expected to increase with the temperature. However, the decrease in the selectivity at the higher temperatures for the La_2O_3, Sm_2O_3, and Eu_2O_3 (when $CH_4/O_2 = 4.0$), is attributed mostly to the conversion of methyl radicals to CO and CO_2 on the catalyst surface. To a small extent, it may also be due to combustion ethane and ethylene in gas phase and/or on the catalyst surface at the higher temperatures.

In all the cases, the ethylene/ethane ratio in the products is found to increase with increase of the temperature and decrease of the CH_4/O_2 ratio. The increase in the ethylene/ethane ratio is probably because of the availability of O_2 at higher concentration for the following gas-phase reactions involved in the formation of ethyl radicals and ethylene from ethane (*14, 15*).

$$C_2H_6 + O_2 \rightarrow C_2H_5. + HO_2. \quad (2)$$

$$C_2H_5. + O_2 \rightarrow C_2H_4 + HO_2. \quad (3)$$

$$C_2H_6 + HO_2. \rightarrow C_2H_5. + H_2O_2 \quad (4)$$

$$H_2O_2 + Z \rightarrow 2\,OH. + Z \quad (5)$$

(where Z is a third body, e.g., water molecule).

$$C_2H_6 + OH. \rightarrow C_2H_5. + H_2O. \quad (6)$$

Ethane is formed by gas-phase coupling of methyl radicals (*13*).

The increase in the ethylene/ethane ratio with the temperature is expected due to the decomposition of ethyl radicals and thermal cracking of ethane at the higher temperatures as follows:

$$C_2H_5. \rightarrow C_2H_4 + H. \quad (7)$$

$$C_2H_6 \rightarrow C_2H_4 + H_2 \quad (8)$$

It may also be due to the increase in the rate of the gas-phase reaction for the conversion of ethyl radicals to ethylene (Reaction 3) and due to the oxidative dehydrogenation of ethane on the catalyst surface.

The CO/CO_2 ratio in the products is found to be lowest for the CeO_2 and highest for the Yb_2O_3. The very low CO/CO_2 ratios for the CeO_2 are attributed to a rapid conversion of methyl radicals to CO_2 on the catalyst surface; CeO_2 in its pure form is a complete oxidation catalyst (*6*). For the Yb_2O_3, the observed higher CO/CO_2 ratio and its decrease with the temperature (Fig. 9) are attributed to its lower reactivity of Yb_2O_3 with methyl radicals (*6*) and to its increased reactivity at higher temperatures, respectively. In general, the CO/CO_2 ratios observed for the rare-earth oxides catalysts (Fig. 9) are quite consistent with what is expected from their reactivity with methyl radicals (*6*) assuming that surface reaction of methyl radicals leads to formation of mostly CO_2 or to combustion products with CO/CO_2 ratio

TABLE 1

Comparison of the Surface and Catalytic Properties of the Rare-Earth Metal-Oxide Catalysts

Catalyst	Surface area ($m^2 \cdot g^{-1}$)	Chemisorption of CO_2 ($\mu mol \cdot g^{-1}$)		Chemisorption of NH_3 at 373 K ($mmol \cdot g^{-1}$)	Catalytic properties					
		At 323 K	At 773 K		CH_4/O_2 ratio (in feed)	CH_4 conversion (%)	O_2 conversion (%)	C_2 selectivity (%)	C_2 yield (%)	C_2H_4/C_2H_6 ratio
La_2O_3	3.8	91.2	55.9	1.69	4	24.8	93.6	55.5	13.8	1.28
					8	18.2	95.9	69.9	12.7	0.88
CeO_2	3.0	31.8	13.6	0.41	4	16.7	92.6	25.6	4.3	0.82
					8	9.7	94.1	28.3	2.8	0.54
Sm_2O_3	3.9	39.2	4.5	0.38	4	24.0	94.0	48.9	11.7	1.04
					8	16.0	95.0	62.1	9.8	0.78
Eu_2O_3	4.9	77.0	19.6	0.25	4	22.8	94.5	44.5	10.1	1.14
					8	15.2	94.4	58.5	8.9	0.85
Yb_2O_3	1.8	37.5	11.7	1.09	4	12.9	66.3	48.5	6.2	1.20
					8	6.9	77.5	62.0	4.3	0.78

Note. Reaction conditions: amount of catalyst, 0.1 g; feed, mixture of pure methane and O_2; total gas flow rate, 180 $cm^3 \cdot min^{-1}$ (at STP); temperature, 1123 K.

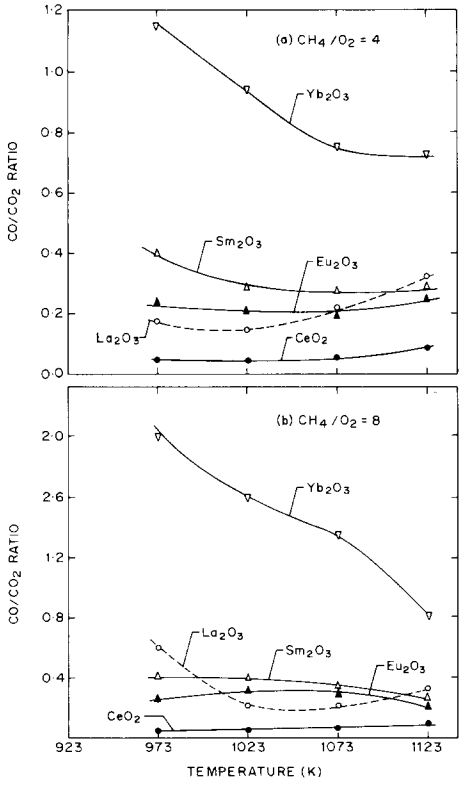

FIG. 9. Dependence of CO/CO_2 ratio in products in oxidative coupling of methane over the rare earth metal oxide catalysts on reaction temperature and CH_4/O_2 ratio.

very much less than 1, whereas in gas-phase reactions, a formation of CO, as compared to CO_2, is much higher (*16, 17*).

Relationship between Surface and Catalytic Properties

Campbell *et al.* (*5*) have indicated that the activities of rare-earth oxides for the abstraction of hydrogen atom from methane molecule to form methyl radical can best be related to basicity of the oxides, the more basic oxides being more active. The comparison of the catalytic activity and selectivity with the basicity of the catalysts shows that the higher methane conversion activity, C_2-selectivity, and C_2-yield observed for the La_2O_3 are consistent with the higher basicity (both the total and strong basicity). However, for the other rare-earth oxides studied their activity and selectivity does not show any trend with the total and strong basicity. A comparison of the orders of the catalysts for their catalytic activity, C_2-selectivity, and C_2-yield with those for their total and strong basicity (Table 1) reveals that basicity of the catalysts alone is not responsible for controlling the catalytic activity and selectivity in oxidative coupling of methane.

It is interesting to note that the order of the catalysts for their acid sites of intermedi-

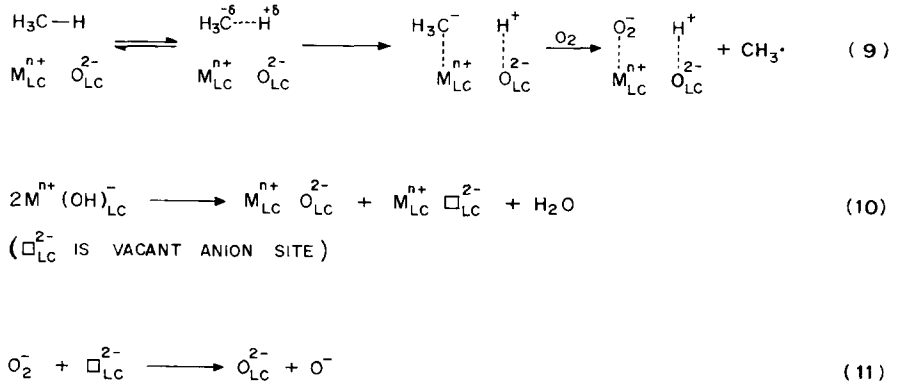

FIG. 10. Formation of methyl radicals involving an acid-base pair on the catalyst surface.

ate strength ($La_2O_3 > Sm_2O_3 > Eu_2O_3 > CeO_2 > Yb_2O_3$) is similar to their order for methane conversion activity and, except for Yb_2O_3, also similar to their order for C_2-selectivity and C_2-yield, whereas the order of the catalysts for their strong acid sites ($Yb_2O_3 > Eu_2O_3 > Sm_2O_3 > La_2O_3$) is different or almost opposite to their order for catalytic activity, selectivity, and yield. The La_2O_3, which contains acid sites of only intermediate strength, showed highest activity and C_2-selectivity (or C_2-yield). The CeO_2 (which contains very strong acid sites) gave poor selectivity and yield for the C_2-hydrocarbons.

From the above observations, it is evident that the methane conversion activity and C_2-selectivity of the catalysts depend not only on their basicity but also on their acidity. Dependence of the catalytic properties on the acidity and basicity is, however, complex. It seems that an acid–base pair (M^{n+}_{LC} O^{2-}_{LC}) on the metal-oxide surface is involved in the abstraction of the H-atom from methane molecule, as shown in Fig. 10. When methane interacts with an acid–base pair having enough strength, it undergoes heterolytic C–H-bond rupture, resulting in CH_3^-- and H^+-ions which interact with the EPA (or acid) site (M^{n+}_{LC}) and the EPD (or base) site (O^{2-}_{LC}), respectively. In the presence of O_2, an electron transfer from the carbanion (CH_3^-) to O_2, resulting in O_2^-, is expected to take place (*18*) and the methyl radical is released in gas phase or oxidized on the catalyst surface. The methyl radicals released in the gas phase can then undergo reactions in the gas phase and over the catalyst surface (*2, 13, 19*).

Lin *et al.* (*2*) have observed that the formation of methyl radicals on La_2O_3 in substantial concentrations, O_2 must be present in the reactant stream, even though the catalyst had been pretreated in O_2. This supports the possibility of the electron transfer from CH_3^- to form O_2^- (Fig. 10) in the formation of methyl radicals. The function of the O^{2-}_{LC} (which is a strong basic site) would be to abstract a proton from the adsorbed CH_4 to form OH^-_{LC}. The anion (basic) site is regenerated by dehydroxylation of the catalyst surface at the high reaction temperature leading to a formation of water (Reaction (10)). There is also a possibility of formation of O^- (which is most reactive among surface oxygen species) on the catalyst surface by Reaction (11). The O^- species formed via O_2^- may further give rise to the formation of methyl radicals from methane by the mechanism similar to that described for Li–MgO catalyst (*13*).

According to the above mechanism the carbanions (CH_3^- or $C_2H_5^-$), hydrocarbon radicals ($CH_3.$, $C_2H_5.$, etc.) and unsaturated hydrocarbons are expected to be strongly adsorbed on the strong acid sites. The

strongly adsorbed species are likely to undergo surface reaction with adsorbed O_2^- and O^- leading to the formation of more combustion products. Indeed this has been observed in the present investigation; the catalyst containing acid sites of higher strengths showed poor C_2-selectivity. For the acid strength, an order of the catalysts is $CeO_2 > Eu_2O_3 > Yb_2O_3 > Sm_2O_3 > La_2O_3$, which is exactly opposite to the order of their C_2-selectivity. This indicates that even a small number of very strong acid sites greatly reduce the catalyst selectivity. It may be noted that the measurements of surface basicity (by STD of CO_2) and acidity by TPD of NH_3) have not been carried out under the actual reaction conditions. Therefore, it is somewhat dangerous to correlate the surface acidity and basicity with the catalytic properties. Nevertheless, the information obtained from this exercise is quite useful for understanding the catalytic process.

CONCLUSIONS

The following conclusions have been drawn from the present investigation on the rare-earth oxide catalysts (viz. La_2O_3, CeO_2, Sm_2O_3, Eu_2O_3 and Yb_2O_3) for their acidity and basicity distributions and their catalytic activity/selectivity in the oxidative coupling of methane.

1. The rare-earth oxide catalysts studied differ widely in their acidity and basicity and in the site energy distribution of both the acid and basic sites. The La_2O_3 showed highest basicity (both the total and strong basic sites) and acidity; its acid sites are, however, of intermediate strength. The acid and base sites on the catalysts are the accessible M^{n+}_{LC} cations and O^{2-}_{LC} anions on the catalyst surface and the site energy distribution of the acid and base sites is mostly attributed to the presence of M^{n+}_{LC} and O^{2-}_{LC} ions in different coordinations, the lower coordinated ion site being responsible for the stronger acid/base sites.

2. Among the rare-earth oxides, the La_2O_3 showed highest activity and C_2-selectivity (or C_2-yield), whereas the lowest C_2-yield and -selectivity are shown by the CeO_2. The C_2-yield by the other catalysts was in the order: $Sm_2O_3 > Eu_2O_3 > Yb_2O_3$.

3. Comparison of the surface acidity/basicity with the catalytic activity/selectivity indicated a complex relationship between the two; surface basicity alone cannot control the catalytic properties. Surface acidity seems to play a very significant role, particularly in deciding the C_2-selectivity. The catalysts having strong acid sites showed poor C_2-selectivity.

4. It seems that an acid–base pair (M^{n+}_{LC} O^{2-}_{LC}) on the surface is involved in the abstraction of the H-atom from absorbed methane molecule by its polarization followed by heterolytic C–H-bond rupture. The resulting CH_3^-- and H^+-ions interact with the acid and base site, respectively. Methyl radical is then formed by an electron transfer from the carbanion ion to O_2, resulting in O_2^-. Stronger acid sites are harmful for the selectivity as they interact strongly with the carbanions and also with hydrocarbon radicals and olefins, favouring surface-catalysed combustion reactions.

REFERENCES

1. Otsuka, K., Jinno, K., and Morikawa, A., *Chem. Lett.*, 499 (1985).
2. Lin, C.-H., Campbell, K. D., Wang, J. X., and Lunsford, J. H., *J. Phys. Chem.* **90,** 534 (1986).
3. Otsuka, K., Jinno, K., and Morikawa, A., *J. Catal.* **100,** 353 (1986).
4. Otsuka, K., and Komatsu, T., *Chem. Lett.*, 483 (1987).
5. Campbell, K. D., Zhang, H., and Lunsford, J. H., *J. Phys. Chem.* **92,** 750 (1988).
6. Tong, Y., Rosynek, M. P., and Lunsford, J. H., *J. Phys. Chem.* **93,** 2896 (1989).
7. Korf, S. J., Roos, J. A., Diphoorn, J. M., Veehof, R. H. J., van Ommen, J. G., and Ross, J. R. H., *Catal. Today* **4,** 279 (1989).
8. Choudhary, V. R., Chaudhari, S. T., Rajput, A. M., and Rane, V. H., *J. Chem. Soc. Chem. Commun.*, 555 (1989); 605 (1989); 1526 (1989).
9. Choudhary, V. R., Chaudhari, S. T., Rajput, A. M., and Rane, V. H., *Catal. Lett.* **3,** 101 (1989).
10. Choudhary, V. R., Chaudhari, S. T., Rajput, A. M., and Rane, V. H., *Res. Ind.* **34,** 258 (1989).

11. Choudhary, V. R., and Rane, V. H., *Catal. Lett.* **4,** 101 (1990).
12. Che, M., and Tench, A. J., *in* "Advances in Catalysis" (D. D. Eley, H. Pines, and P. B. Weisz, Eds.), Vol. 31, p. 77. Academic Press, San Diego, 1982.
13. Ito, T., Wang, J.-X., Lin, C.-H., and Lunsford, J. H., *J. Am. Chem. Soc.* **107,** 5062 (1985).
14. Morales, E., and Lunsford, J. H., *J. Catal.* **118,** 255 (1989).
15. Geisbrecht, R. A., and Daubart, T. E., *Ind. Eng. Chem. Process Des. Dev.* **14,** 159 (1975).
16. Lane, G. S., and Wolf, E. E., *J. Catal.* **113,** 144 (1988).
17. Choudhary, V. R., Chaudhari, S. T., and Rajput, A. M., *AIChEJ.*, revised paper communicated.
18. Garrone, E., Zecchina, A., and Stone, F. S., *J. Catal.* **62,** 396 (1980).
19. Kimble, J. B., and Kolts, J. H., *Energy Prog.* **6,** 226 (1986).